Co-Channel Interference Cancellation at the User Terminal in Multibeam Satellite Systems

G. Cocco[†], M. Angelone[¶] and A.I. Perez-Neira[1,2]

[†]*German Aerospace Center - DLR*
Oberpfaffenhofen, D-82234, Wessling, Germany
[¶]*European Space Agency - ESTEC, Noordwijk – The Netherlands*
[1]*Centre Tecnològic de Telecomunicacions de Catalunya – CTTC*
Parc Mediterrani de la Tecnologia, Av. Carl Friedrich Gauss 7 08860, Castelldefels – Spain
[2]*Department of Signal Theory and Communications*
Universitat Politecnica de Catalunya, Barcelona, Spain
giuseppe.cocco@dlr.de, martina.angelone@esa.int, ana.perez@cttc.es

SUMMARY

We study the applicability of soft interference cancellation in the forward link of multibeam satellite systems with focus on mobile terminals. We adopt a standard currently used in commercial satellite systems as a reference. The multibeam satellite antenna radiation diagram has been generated using a physical optics reflector model while a widely adopted channel model has been used for the land mobile satellite (LMS) channel. The interference pattern has been derived using a system simulator developed by the European Space Agency (ESA). Starting from the analysis of the interference pattern we study the application of a low complexity soft interference cancellation scheme for commercial applications. Our results show that, under realistic conditions, a two-colors frequency reuse scheme can be employed while guaranteeing service availability across the coverage and keeping the complexity at the user terminals relatively low. Copyright © 2013 John Wiley & Sons, Ltd.

1. INTRODUCTION

Frequency spectrum scarcity is one of the main capacity-limiting factors in wireless communication systems. A common practice to overcome bandwidth shortage in both satellite and terrestrial networks using multiple beams/cells consists in dividing the available spectrum into non overlapping sub-bands (colors) and reuse them over non-adjacent geographical regions. Coloring schemes with a small number of colors allow for a more efficient utilization of the spectrum resources, but have the drawback of increasing the co-channel interference (CCI) due to the non-ideal antennas radiation patterns. Despite the improvements in antennas technology, undesired side lobes are still a particularly challenging problem in geostationary (GEO) satellite communications, since the interference coming from co-channel beams can heavily affect the reception of the desired signal at the user terminal such that either the link throughput or the availability are penalized. This problem is exacerbated by the use of aggressive frequency reuse patterns. Interference cancellation techniques at the user terminal (UT) represent a possible solution to this problem. Many different interference cancellation techniques have been proposed up to date. A comprehensive overview is presented in [1]. From an information theoretical point of view the problem of CCI can be

*Prepared using *satauth.cls* [Version: 2010/05/13 v2.00]*

studied starting from the multiple access channel (MAC) [2] model [*]. The capacity of the MAC channel can be achieved by decoding each of the signals individually starting from the strongest one (which, in many practical applications, is the useful or *reference* signal) and performing successive interference cancellation (SIC) under the hypothesis of Gaussian signalling. In a real system the interfering signals can be approximated as Gaussian noise in some cases. This approximation is justified by the Central Limit Theorem if the number of interfering signals is sufficiently high and they have similar powers. In satellite systems with high frequency reuse it is often the case that a relatively small number of interferers have power comparable to that of the reference signal, while the others are much weaker. In this case the Gaussian approximation may not be accurate. A more suitable approach is to consider the actual statistics of the interfering signals provided that some basic knowledge of the main interferers, such as channel state information and modulation type, is available. One option is to adopt a maximum a posteriori (MAP) symbol detector. Such detector has the drawback of having a complexity that grows exponentially with the number of signals to detect. In order to keep complexity low, while trading part of the performance, several simplified schemes have been proposed in literature such as [3], [4] and [5]. Iterative decoding has been shown to achieve the multiple access channel (MAC) capacity in [6], by integrating error control coding with multiple access interference suppression. In [7] two iterative low complexity algorithms for adjacent channel interference (ACI) cancellation in satellite systems are presented. In [8] the authors proposed a parallel multi-user detector for adjacent channel interference cancellation in the return link of Inmarsat's Broadband Global Area Network (BGAN) system.

In the present paper we study the applicability of soft co-channel interference cancellation in the forward link of a satellite system with high frequency reuse based on a realistic scenario, with focus on mobile terminals. The results presented here have been developed within the Advanced Research in Telecommunications Systems (ARTES) project Next Generation Waveform for Increased Spectral Efficiency (NGWISE) funded by the European Space Agency (ESA) [9]. The standard adopted in the European Telecommunications Standard Institute (ETSI) Satellite Component of UMTS (S-UMTS) [10] has been used as a baseline. The multibeam satellite antenna radiation diagram has been generated through a commercial software used for satellite antenna design and analysis, while the interference pattern has been calculated using a system simulator developed by ESA. A widely used channel model has been adopted for the land mobile satellite (LMS) channel. Unlike most of previous works, we start from the analysis of the interference distribution across the coverage area. Based on the interference distribution we propose an interference management solution based on iterative soft interference cancellation. It is worth noting that our work differs from [7] and [8] in that co-channel rather than adjacent channel interference is considered. In fact, whenever standard channel spacing is considered [†] and an aggressive frequency reuse scheme is applied, indeed CCI becomes the most relevant source of interference in the system as its level is much higher with respect to that of the ACI. Unlike in [8] we consider the forward link rather than the return link. Interference cancellation in the forward link is constrained by the complexity at the UT, especially in the LMS context. We show that, assuming a realistic interference distribution across the coverage, the optimal detector can be applied at the receiver with affordable complexity if the same symbol rate is kept across all co-channel signals coming from the satellite. Our results show that frame error rates as low as 10^{-3} can be achieved in the whole covered area while using a two-color frequency reuse scheme. Such a high frequency reuse can lead to a potential increase in spectral efficiency with respect to coloring schemes usually adopted in commercial satellite systems. Furthermore, we study the effect of signals misalignment at the satellite showing that misalignment errors can be tolerated up to a certain extent.

The rest of the paper is organized as follows. In Section 2 the system model is presented while in Section 3 we describe the proposed solution specifying the required modifications to ETSI

---

[*]The problem could also be studied from an information theoretical perspective as a broadcast channel or an interference channel depending on the specific system studied [2]

[†]this may not be the case if techniques such as time-frequency packing are applied [11]. However, this falls out of the scope of the present work.

Int. J. Satell. Commun. Network. (2013)

standard [12]. In the same section we perform a preliminary evaluation of the proposed interference cancellation method. The numerical results are presented in Section 4 while Section 5 summarizes the main contributions of the paper.

2. SYSTEM MODEL

We consider the forward link of an interactive geostationary (GEO) multibeam satellite system with 210 user-link beams operating in L/S band. Each beam occupies half of the available user-link bandwidth and a two-color frequency reuse pattern is adopted, with a single polarization per beam. The coloring scheme is such that the same color is used in beams along the same parallel while colors alternate along meridians.

Due to the satellite antenna radiation pattern each beam suffers from the interference generated by the closest co-channel beams. As shown in Figure 1 the red color identifies the reference beam while orange is used for the co-channel interfering beams. In order to be representative of the best case and the worst case scenarios we considered two beams for our analysis, namely beam 105 and beam 110, one at the center and one at the edge of the global coverage, respectively.
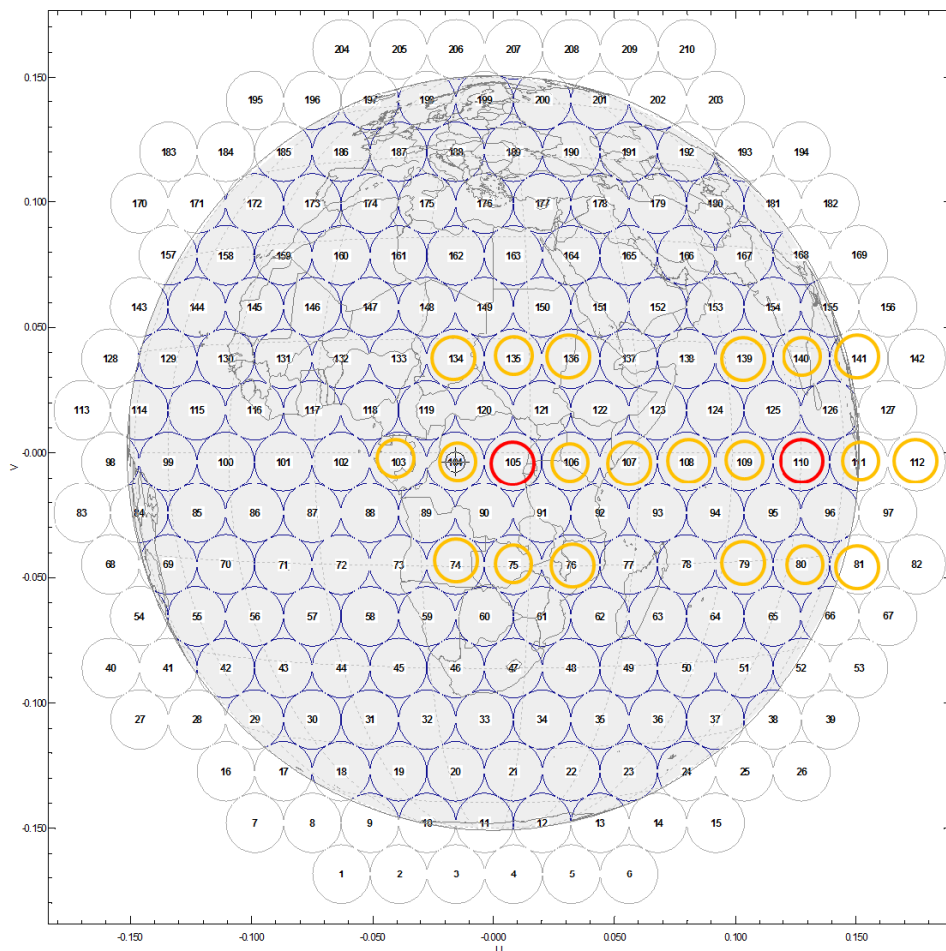

Figure 1. Considered reference and interfering beams and conventional numbering. Reference and interfering beams are shown in red and yellow, respectively.

Considering a UT in a given beam we refer to the desired signal as *reference signal*. We assume that terminals are equipped with a single antenna and that only one polarization is used. No spreading is assumed on the signal.

The received signal at time t when N_{int} interferers are present is:

$$y(t) = h(t) \left[g^C(t) x^C(t) + \sum_{n_{int}=1}^{N_{int}} g^I_{n_{int}}(t_{n_{int}}) x^I_{n_{int}}(t_{n_{int}}) \right] + n(t), \qquad (1)$$

where $t_{n_{int}} = t - \tau_{n_{int}}$, $\tau_{n_{int}}$ being the time offset of interferer number n_{int} with respect to the reference symbol, while

$$g^I_{n_{int}}(t) = G^I_{n_{int}} e^{j(2\pi\Delta\nu_{n_{int}}t + \varphi_{n_{int}})}, \qquad (2)$$

$G^I_{n_{int}}$ being the antenna gain of the co-channel interfering beam n_{int} in the direction of the UT, normalized to the gain of the reference signal, while $\Delta\nu_{n_{int}}$ and $\varphi_{n_{int}}$ are the frequency and phase offsets with respect to the local oscillator at the UT, respectively. Similarly we defined

$$g^C(t) = G^C e^{j(2\pi\Delta\nu_C t + \varphi_C)}, \qquad (3)$$

with $G^C = 1$.

Signals $x^C(t)$ and $x^I_{n_{int}}(t)$, $n_{int} \in \{1, \ldots, N_{int}\}$, are the reference (i.e., the desired one) and the interfering signals, respectively. The interfering signals (and similarly the reference one) can be expressed as

$$x^I_{n_{int}}(t) = \sum_{l=1}^{N^{CW}_{N_{int}}} s_{n_{int}}(l) g(t - l T^{n_{int}}_s), \qquad (4)$$

where $g(t)$ is a root-raised cosine pulse with roll-off α, $s_{n_{int}}(l)$ represents the $l-th$ received symbol from interferer n_{int}, $T^{n_{int}}_s$ is the symbol duration while $N^{CW}_{n_{int}}$ is the number of modulated symbols in a codeword for interferer n_{int}. The term $h(t)$ in Eqn. (1) takes into account the channel effect (phase rotation and propagation loss). Note that $h(t)$ is a common multiplying factor for all signals, since all waveforms originate from the same spacecraft and in the forward link all signals cover the same path to the UT. We assume that the maximum frequency offset is such that $\Delta\nu_{n_{int}} T_S \ll 1/100$, $\forall n_{int} \in \{1, \ldots, N_{int}\}$. The sample taken at time t_k after matched filtering and sampling of signal $y(t)$ is:

$$y_k = h(t_k) \left[g^C(t_k) s(k) + \sum_{n_{int}=1}^{N_{int}} g^I_{n_{int}}(t^{n_{int}}_k) \sum_{l=1}^{N^{CW}_{n_{int}}} s_{n_{int}}(l) g(t^{n_{int}}_k - l T^{n_{int}}_s) \right] + w_k, \qquad (5)$$

where $t^{n_{int}}_k = t_k - \tau_{n_{int}}$ while w_k's are independently and identically distributed (i.i.d.) zero mean complex Gaussian random variables with variance σ^2 in each component. The interfering signals gains $G^I_{n_{int}}$ depend on the satellite antenna radiation pattern. Thus, the use of a realistic antenna pattern is of fundamental importance for the selection and the performance assessment of an adequate interference cancellation technique at the UT. In the following we give details about the antenna pattern and the system model used in the present paper.

2.1. System Simulations and Antenna Pattern Models

This section describes the system simulator used to compute the interference pattern as well as the models used to create the considered antenna pattern.

The ESA satellite communication systems analysis tool, developed in MATLAB, performs a multi-dimensional space-time link budget over a uniform latitude-longitude grid of users, averaging over a user-defined set of time availabilities with the related attenuations and probabilities. The

reference propagation models are based on ITU recommendation [13] and it is assumed that the traffic request among different beams is uniform. For the sake of this study we focus on clear sky conditions, since atmospheric attenuation does not represent a serious impairment in L/S band. Each user of the grid is assigned to a specific beam if the gain of such beam in its location is the highest across the coverage. Then, based on the frequency plan and on the consequent beam coloring, the resulting interference pattern and distribution are calculated. The simulated system foresees the use of Adaptive Coding and Modulation (ACM) that enables each user to select the most efficient modulation and coding (ModCod) scheme allowed by the link condition. In general the ACM in LMS systems is more challenging with respect to the case of fixed terminals due to the rapid changes in the communication channel induced by the terminal motion. In [12] a return channel is used to feed-back the measured SNR (or SINR) to the Bearer Control Layer. The information is used at the control unit to select the bearer according to a target QoS. Such system is used to adapt the communication rate to the long-term channel variations only, since short-term fading is covered by the link margin [12, Section 7]. Further analysis in the implementation of the ACM mechanism is out of the scope of this paper.

The downlink signal-to-interference ratio (in linear scale) in the point x belonging to beam i is given by:

$$\left(\frac{C}{I}\right)^{DL}_{co}(x) = \frac{P_{TX\_SAT}(i)G^{sat}_{TX_{co-po}}(i,x)}{\sum_{j=1,j\neq i}^{N_{co-ch}} P_{TX\_SAT}(j)G^{sat}_{TX_{co-po}}(j,x)}, \tag{6}$$

where:

- $P_{TX\_SAT}(i)$ is the saturated power per carrier of beam i
- $G^{sat}_{TX_{co-po}}(i,x)$ is the co-polar satellite TX antenna gain of beam i in the location x
- $P_{TX\_SAT}(j)$ is the saturated power per carrier of beam j; in the following it is assumed that all the carriers have equal power and therefore this term can be assumed to be a constant
- $G^{sat}_{TX_{co-po}}(j,x)$ is the co-polar satellite TX antenna gain of co-channel beam beam j in the location x.

We assume that solid state power amplifiers (SSPAs) are used on-board the satellite payload. In this analysis we focus on the first N_{co} strongest interferers received at the user terminal and define for each of them:

$$\left(\frac{C}{I_j}\right)_{co}(x) = \frac{G^{sat}_{TX_{co-po}}(i,x)}{G^{sat}_{TX_{co-po}}(j,x)}, \tag{7}$$

as the signal to co-channel interference related to the j-th co-channel interferer, assuming that $I_j \geq I_{j+1} \; \forall j \in \{1,\ldots,N_{co}\}$ and $I_{N_{co}+1} = 0$. As for the considered antenna pattern, a commercial software for antenna design analysis and coverage planning has been used to reproduce a beam pattern similar to the one of a commercial satellite system [14]. The software is based on physical optics reflector modeling and allows for accurate characterization of the directivity of both the co-polar and the cross-polar fields, as well as scan-aberrations and losses [15]. A geostationary satellite in the 25 deg East orbital position has been considered. The ETSI standard [12] was considered for the PHY layer

The reflector has been modeled with the parameters listed in the following table:

Parameter	Value
Aperture size [m]	9
F/D	1.34
Beam spacing/θ 3dB [deg]	1.363
Crossover Level [dB]	-3
Aperture Efficiency	59.1%
Directivity [dBi]	40.85

The resulting beam pattern gain is plotted in Figure 2, where the coverage has been filtered with a relative threshold of -4.5 dB with respect to the peak gain, which means that all the users with a gain lower than 4.5 dB with respect to the peak gain have not been considered.
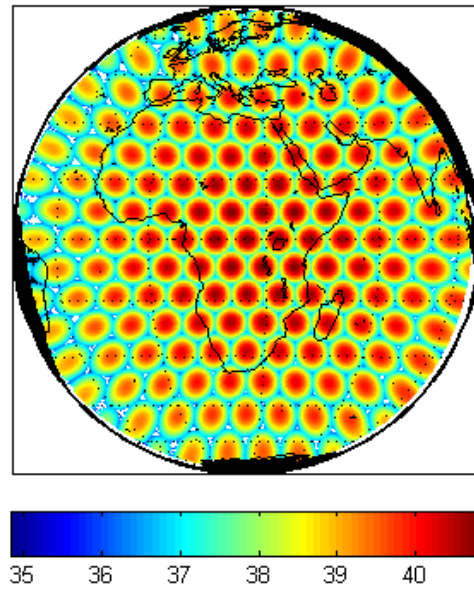
Figure 2. Antenna beam pattern gain [dBi].

3. PROPOSED SOLUTION

We consider the forward bearers family of the standard [12]. We aim to find an interference cancellation solution at the UT that is at the same time efficient and that has low complexity. We propose to split the complexity between system and UT levels. In the following the modifications required at system level with respect to the standard are detailed.

3.1. System Level

The modifications that would be required to [12] are hereafter specified and the related implications and feasibility discussed.

1. It is assumed that the symbol rate $R_s^I = 1/T_s^I$ of the strongest interferer is the same as that of the reference signal $R_s^C = 1/T_s$, T_s being the symbol period of the reference signal. Although in principle different channel code rates, modulations and FEC block sizes may be used in the two signals, the simulation results we present in Section 4 show that there are some restrictions on the modulations and code rates that can be adopted. Note that assuming the same symbol rate for the reference and the interfering signals implies $T_s^{n_{int}} = T_s$, $\forall n_{int} \in \{1, \ldots, N_{int}\}$, in expression (5).

2. The symbols of reference and interfering signals are aligned such that the intersymbol interference (ISI)-free sample instants of the reference signal correspond to the ISI-free sample instants of the interferer, which implies $\tau_{n_{int}} = 0 \, \forall n_{int} \in \{1, \ldots, N_{int}\}$ in expression (5). However, in Section 4 we show that this constraint can be relaxed up to a certain extent.

3. The receiver knows the modulation used by the interferer. This information can be made available to the UT through the global beam and using knowledge of the user position, which is currently foreseen in [12] through the GPS signal. Knowing the position with respect to the reference beam, a user could derive which is the strongest interfearing beam. The information about the modulation used in each beam (and thus also in the interfearing beam) during a given time slot is transmitted over the global beam. We use this assumption as it simplifies the

description of the proposed scheme, although in Section 4 we will show that it can be actually removed.

3.2. Iterative SISO Decoder at the User Terminal

We assume that the channel of both the reference signal and the strongest interferers as well as the ISI-free sample instants of the reference signal can be estimated. This assumption is usually taken in most multi-user detection (MUD) systems. Channel estimation can be performed using the pilot symbols inserted at regular intervals in the frame as foreseen in [12]. In case the pilot symbols of reference and interfering signal overlap, joint estimation methods may be adopted (e.g., E-M algorithm [16])[‡]. An extensive literature is available on the subject and further analysis is out of the scope of this paper. We further assume that conditions $1 \rightarrow 3$ described in Section 3.1 hold.

In case no interference is present, in a typical receiver the turbo decoder is fed with the log-likelihood ratio (LLR) vector of the sampled received signal. Let R be the channel code rate. The m_b-th component, $m_b \in \{1, \ldots, RN_C^{cw}\}$ of the LLR vector for QPSK signalling and using the Grey mapping scheme of [10] can be expressed as:

$$LLR_{m_b} = \log\left(\frac{Pr\{b_{m_b} = 1 \,|y_k\}}{Pr\{b_{m_b} = 0 \,|y_k\}}\right) = \log\left(\frac{P_{k,s_2} + P_{k,s_3}}{P_{k,s_0} + P_{k,s_1}}\right), \tag{8}$$

for $m_b = 2k - 1$, while

$$LLR_{m_b} = \log\left(\frac{P_{k,s_1} + P_{k,s_3}}{P_{k,s_0} + P_{k,s_2}}\right), \tag{9}$$

for $m_b = 2k$, where P_{k,s_n} is the probability to observe the sample y_k conditioned to the transmission of the symbol s_n, $n \in \{0, 1, 2, 3\}$, while b_{m_b} indicates the m_b-th coded bit in the transmitted codeword. Eqn. (8), and similarly Eqn. (9), is derived taking into account that, according to the considered mapping, symbols s_2 and s_3 correspond to a bit pair with the first bit equal to 1, while the first bit of the pair mapping to s_0 and s_1 is equal to 0. Eqn. (8) can be easily extended to the case of 16 QAM modulation. The probability P_{ks_n} is proportional to:

$$P_{k,s_n} \propto \exp\left\{\frac{|y_k - h(t_k)G^C s_n|^2}{2\sigma^2}\right\}. \tag{10}$$

In the case of a single interferer with constellation size M, the probability that the k-th symbol of the reference signal $s(k)$ is equal to s_n can be expressed as:

$$P_{k,s_n} = \sum_{m=0}^{M-1} P_{s_m^I} P_{k,s_n,s_m^I}, \tag{11}$$

where P_{k,s_n,s_m^I} represents the probability to receive y_k conditioned to symbols s_n and s_m^I in the reference and in the interfering signals, respectively, while $P_{s_m^I}$ represents the probability of transmitting symbol s_m^I, which is assumed to be equal to $1/M$. The probability P_{k,s_n,s_m^I} is proportional to:

$$P_{k,s_n,s_m^I} \propto \exp\left\{\frac{|y_k - h(t_k)g^C(t_k)s_n - h(t_k)g_{n_{int}}^I(t_k)s_m^I|^2}{2\sigma^2}\right\}. \tag{12}$$

This can be easily extended to the case of a generic number of interferers N_{int} each with its phase and frequency offsets and amplitude, leading to the following expression for the optimal symbol

---

[‡]A similar problem has been addressed in [17] and [18] where the feasibility of the joint estimation of phase, amplitude and frequency offsets of colliding signals is studied.

detector,

$$P_{k,s_n} = \sum_{m_1=0}^{M_1-1} \cdots \sum_{m_{N_{int}}=0}^{M_{N_{int}}-1} \prod_{j=1}^{N_{int}} P_{s_j^I} P_{k,s_n,s_{m_1}^I,\ldots,s_{m_{N_{int}}}^I}, \tag{13}$$

where $M_{n_{int}}$ is the constellation size of interferer number n_{int}. The complexity of expression (13) grows exponentially with the number of interferers.

Once the a-priori probabilities for the desired signal have been derived they can be used to calculate the L-values that are fed to the turbo decoder. In this case the only modification at the receiver side with respect to the standard terminal is limited to the signal detector, while no modification would be needed to the decoder. The performance of the receiver in terms of FER (and potentially in terms of throughput, as higher ModCods could be adopted) can be further improved through an iterative detection-decoding scheme. The iterative process can be implemented as done in the benchmark system of [3, Fig. 1], in which the receiver at each iteration jointly detects all the received signals in a parallel fashion and then feeds the a-priori probability for each of them to a distinct decoder after subtracting the intrinsic information. We opted for a scheme which is more suited for an implementation with a single decoder, namely a joint soft input-soft output (SISO) detector with serial decoding, which is shown in Fig. 3. In the figure the block diagram describing one detection-decoding iteration is shown for the case of two interferers. Signals are detected in decreasing order of strength. Each iteration consists into the following steps. First the detector calculates the L-value L_j for the reference signal and passes it to the turbo decoder. The decoder outputs a soft estimation of the channel symbols relative to the desired signal (P_{k,s_n} in the figure). Such estimation is then fed again to the detector together with the channel output and an estimation of the first (i.e. the most powerful) interferer is obtained. The educated guess obtained so far for the symbol probabilities of the reference signal and the first interferer are then fed to the detector together with the channel output in order to estimate the second interferer. At this point the second iteration starts with the detector using at each step the updated estimates of the symbol probabilities.

Note that, although in Fig. 3 three detectors and three decoders are shown, a single detector/decoder can be used in practice. Note also that in the proposed scheme the decoding step within a given iteration can not be done in parallel as in [3], because each decoding stage uses the output of the previous one. However a parallel decoding would require as many decoders as the number of signals to decode, with a significant increase in complexity and cost of the UT that, especially for mobile users, may be harmful from both an implementation and an economical point of view. Moreover, as shown further in this section, although the time required by one iteration of the proposed scheme is larger with respect to a parallel one, the serial scheme has a faster convergence. This translates in a reduced number of iterations required to achieve a target performance.

In Fig. 4 the FER attained with the soft successive interference cancellation described so far is shown for the case of two interferers. The C/I relative to the first interferer (interferer #1) is 0 dB, i.e., it has the same power of the received signal, while the C/I relative to the other interferer is 6 dB, for a global C/I of -0.9732 dB. The "no MUD" curve in the figure has been derived by treating the interferers as noise and increasing the value of the estimated noise variance passed to the turbo decoder accordingly. The second interferer has a worse FER with respect to the other signals, due to its higher C/I. A 0.8 dB gain can be observed when passing from 1 to 10 detection/decoding iterations for the reference signal. Note that the case with 1 iteration corresponds to the case in which the good signal is detected and decoded only once. This means that the only modification needed at the receiver involves the detector, the complexity of which may be affordable if the number of relevant interfering signals is limited. The distribution of the interferers across the beam will be considered in the next section.

For the case of one interfering signal the gain in the number of iterations of the proposed method with respect to the parallel scheme used as benchmark in [3] can be easily calculated. Let n_{ser} be the number of iterations needed to achieve a certain performance with the proposed scheme and n_{par} be the number of iterations a parallel scheme requires to achieve the same performance. In case of
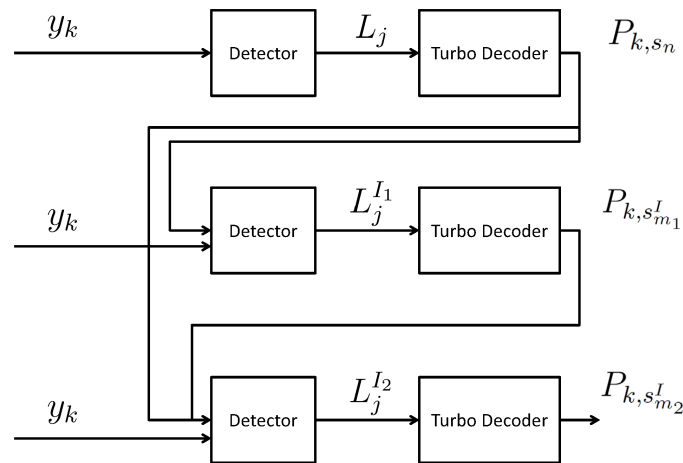
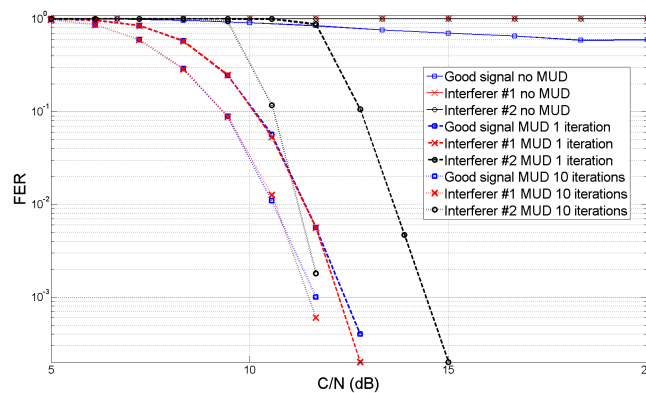Figure 3. Block diagram illustrating an iteration of the SISO detector/decoder.

Figure 4. FER curves for the reference signal and for two interferers. The interferers have a relative C/I of 0 and 6 dB, for a global C/I of -0.9732 dB. A bearer with QPSK modulation, rate 1/3 and 360 data bits per FEC codeword have been used for all signals.

two colliding signals, the following holds:

$$n_{par} = 2n_{ser} - 1, \tag{14}$$

in other words, the proposed method requires roughly half the number of iterations of a parallel method. This can be seen from Fig. 6, where the iterative detection/decoding process is shown for the two methods. 5 iterations for the parallel scheme and three iterations for the proposed one are shown. The red lines indicate the flow of the a-priori probabilities (APPs) calculated by the decoder (reference signal in the upper decoder and interfering signal for the lower one). The input to the detector/decoder is the same for the two considered schemes and consists of the APPs calculated in the previous iteration plus the channel output.

It can be easily shown that such APPs have the same expressions in both schemes by comparing equations (11), (12) and (13) with Eqn. (23) in [3].

Considering that, as previously observed, the extrinsic information passed to each decoder in [3] is equal to the output of the detector in our scheme, the output of the iterative process marked with a red curve in the two schemes of the figure is exactly the same, although only three iterations of the proposed scheme are used versus five of the parallel scheme. Let us now consider the convergence speed. From Fig. 6 it can be seen that a whole iteration of the serial scheme with a single decoder (i.e., estimate both the reference and the interfering signal) takes twice the time of the parallel

decoder with two decoders. Note also that, if we are only interested in the reference signal, only half of the last iteration (skipping the estimation of the interferer) of the serial scheme is needed. Let us indicate with T_{ser} and T_{par} the time spent for an iteration in the two schemes, keeping in mind that $T_{ser} = 2 \times T_{ser}$ and using equivalence (14), it can be seen how the two schemes achieve the same performance in the same time but with just one decoder for the serial scheme while two are required for the parallel scheme.

For the case of more than two signals still a gain in terms of the number required iterations can be observed although deriving a relationship such as one in Eqn. (14) is not straightforward. In the following subsection we present a numerical validation of Eqn. (14).

3.2.1. Optimality Gap In the following we study the gap between the performance of the proposed scheme and a theoretical bound. More specifically, for a given ModCod we fix a target FER which can be considered to be low enough for the system under study (i.e. 10^{-3} according to [19]) and measure the gap, in terms of C/N, between the SNR required by our scheme to achieve the target FER and the minimum SNR required to decode a message with the same rate according to the Shannon bound [2]. We consider the bearer F80T025Q1B-L8 (QPSK, rate $1/3$) in AWGN. Thus, the transmission rate on the channel is $2/3$ bits per channel use (bpcu).

The gap with respect to the theoretical bound is due to two factors. One is the sub-optimality of the physical layer adopted in the standard (e.g., finite codeword length, non-Gaussian signalling [§]), while the other is the sub-optimality of the proposed method. In the following we focus on assessing the entity of this second factor. We start by evaluating the gap due to the code sub-optimality. According to [21] a message with rate $2/3$ bpcu transmitted over an AWGN channel can be decoded with high probability if and only if the following holds:

$$\log_2 \left(1 + \frac{C}{N} \right) \geq \frac{2}{3}, \tag{15}$$

which imposes the following condition on the SNR:

$$\frac{C}{N} \geq 2^{2/3} - 1 = 0.5874 \approx -2.3 \text{ dB}. \tag{16}$$

The physical layer described in [10] for the considered ModCod requires a C/N of about 0.2 dB in order to achieve a FER of 10^{-3} (see Fig. 5). This means that the code loses about 2.5 dB with respect to the theoretical bound.

Now let us consider the case in which two signals are transmitted with the same power C over an AWGN channel. In the system under study the receiver is interested in decoding only one of the two messages. According to the results and under the assumptions relative to the corner points of the capacity region of the MAC channel and the degraded broadcast channel [2], the optimal strategy for a receiver interested only in the strongest signal is to treat the interferer as noise. In such case the receiver can decode successfully the desired message if and only if:

$$\log_2 \left(1 + \frac{C}{N + C} \right) \geq \frac{2}{3}, \tag{17}$$

which leads to:

$$\begin{aligned} \frac{C}{N} &\geq \frac{2^{2/3} - 1}{2 - 2^{2/3}} \\ &= 1.4237 \approx 1.5 \text{ dB}. \end{aligned} \tag{18}$$

[§]In the performance assessment of real codes the modulation-constrained capacity is often used [20]. Here we consider the more general formulas for the AWGN channel capacity since we do not aim at assessing the goodness of the considered channel coding and modulation scheme, but rather to evaluate the incremental gap introduced by the proposed scheme.
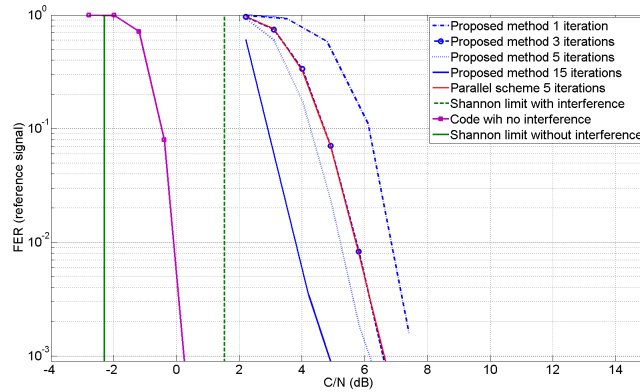
Figure 5. FER in AWGN, QPSK rate $1/3$ used in all signals. The Shannon limit for the case of no interference and for the case with one interferer with $C/I = 0$ dB are also shown. The FER for a scheme in which the signals are decoded in parallel rather than serially (as in the proposed scheme) is also shown. It can be seen how the loss of the proposed scheme with respect to the Shannon limit for a FER of 10^{-3} is only slightly larger than the loss due to the code (curves in case of no interference). It can be also seen how the parallel scheme requires more iterations with respect to the proposed scheme.
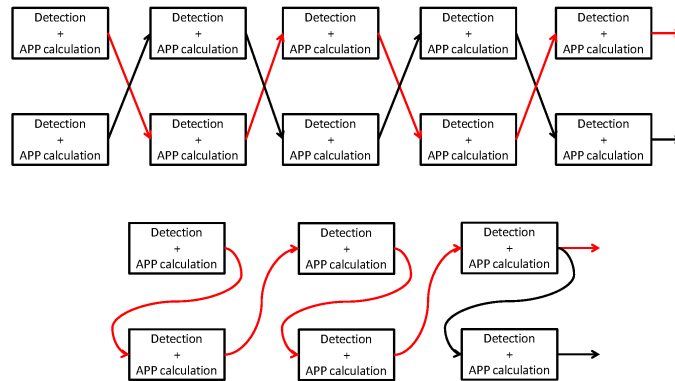
Figure 6. Comparison between the proposed method and a parallel MUD scheme. In red we put into evidence the decoding path for the reference signal. In the figure we show only the propagation of the APPs. In the practical implementation of both schemes the detector takes as input also the received signal, not indicated for sake of clarity.

The proposed scheme achieves the target FER in case of a single interferer at an SNR of about 4.8 dB with 15 iterations, with a loss of 3.3 dB with respect to the theoretical bound, as shown in Fig. 5. Although the loss may seem significant, we note how it is only 0.8 dB larger than the loss due to the code in the case of no interference. This suggests that the total loss of 3.3 dB is mainly due to the non-ideal physical layer and only to a relatively minor extent to the proposed scheme, which results to be highly efficient if enough iterations are allowed. The loss due to the proposed scheme may be further reduced by increasing the number of iterations. Note that the considered bearer has a burst length of 544 symbols, which is relatively short if compared to other standards. Using more powerful channel codes would significantly reduce the gap due to the specific physical layer considered although would increase latency and memory requirements at the UT. In Fig. 5 the FER for a scheme in which the signals are decoded in parallel within an iteration rather than serially (as in the proposed scheme) is also shown.

It can be seen how the parallel scheme requires more iterations with respect to the proposed serial scheme, in accordance with Eqn. (14). As previously mentioned, for a fair comparison, we point out that one iteration of the proposed scheme takes twice the time of one iteration in the parallel scheme. Thus, according to Fig. 6 exactly the same time is required to obtain the same performance in both

schemes. This means that our scheme achieves the same convergence speed of the parallel one using a single decoder rather than two, with an important saving in terms of terminal complexity.

4. NUMERICAL RESULTS

In the following we evaluate the performance of the proposed algorithm for the scenario described in Section 2.

We start by describing in detail the reference scenario and the interference distribution generated by the system level simulator presented in Section 2. The beam numbering and geographical location are shown in Fig. 1. In Table I we show the C/I related to each of the 10 strongest interferers for both beam 105 and 110 in two points, namely at the center of the beam (CoB) and at the edge of the beam (EoB).

Table I. Table with four samples of the interference pattern. Each row contains the C/I related to the ten strongest interfering signals for either a center-of-beam (CoB) point or an edge-of-beam (EoB) point in beams 105 and 110. The total C/I is also reported for each case [19].

| Beam		C/I [dB]										C/I Total [dB]
		1	2	3	4	5	6	7	8	9	10	
105	CoB	37.1107	21.5885	32.1618	37.2214	17.9294	14.5272	27.3961	31.9697	20.7406	29.2564	11.46467
	EoB	15.6046	15.5337	29.8048	15.8007	0.3881	15.1211	21.4581	44.3936	38.1297	21.875	-0.17835
110	CoB	30.3903	19.541	32.9636	35.0503	13.7636	12.1374	21.4154	29.4771	18.9879	30.8531	8.607253
	EoB	27.2207	29.9124	22.4402	17.9726	0.1185	11.5821	18.8873	14.2254	15.2343	27.9627	-0.6047
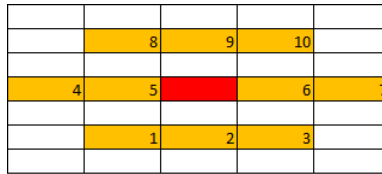
Figure 7. Interference pattern and conventional numbering of the co-channel beams. The central red rectangle represents the reference beam, while the yellow rectangles represent the ten strongest interfering beams.

The numbering relative to the interferers is given according to Figure 7, where the central rectangle represents the reference beam while the yellow rectangles represent the strongest co-channel interferers.

With reference to Table I, it can be seen that in the EoB cases the power of the interferer number 5 is comparable to that of the reference signal while the second strongest interferer is attenuated more than 11 dB. On the other hand, in the CoB the strongest interferer is at least 12 dB lower than the reference signal. Let us consider the worst case scenario, i.e., the EoB. In this case there is only one strong interferer plus nine interferers with a relatively weak power, that, by the Central Limit Theorem, can be modeled as Gaussian noise. Trying to apply MUD to these low-power interferers is not likely to have a relevant impact on the system performance while it would increase significantly the complexity of the receiver. A better choice is to apply the MUD to the desired signal and the strongest interferer while treating the rest of the interferers as noise. In order to understand whether the assumption of having at most one significant interferer is realistic in each point of the beam footprint, we analyzed the distribution of the total C/I across the whole beam. The distribution is shown in Fig. 8, where three cases have been considered for each point in the two beams: i) all the interferers are present (top-left), ii) only the first strongest interferer has been removed (bottom-left) iii) the first two strongest interferers have been removed (bottom-right). From the figure it can be seen that the total C/I reaches negative values, in logarithmic scale, in some areas of the beam (e.g., in the EoB points considered in the table shown in Table I) when all the interferers are present. Removing the strongest interferer determines a minimum C/I *larger than or equal to* 6 dB in any point of the two considered beams. We further notice that the cancellation of the second strongest interferer further increases the minimum C/I of only about 1-1.5 dB. From the analysis of Fig. 8 we
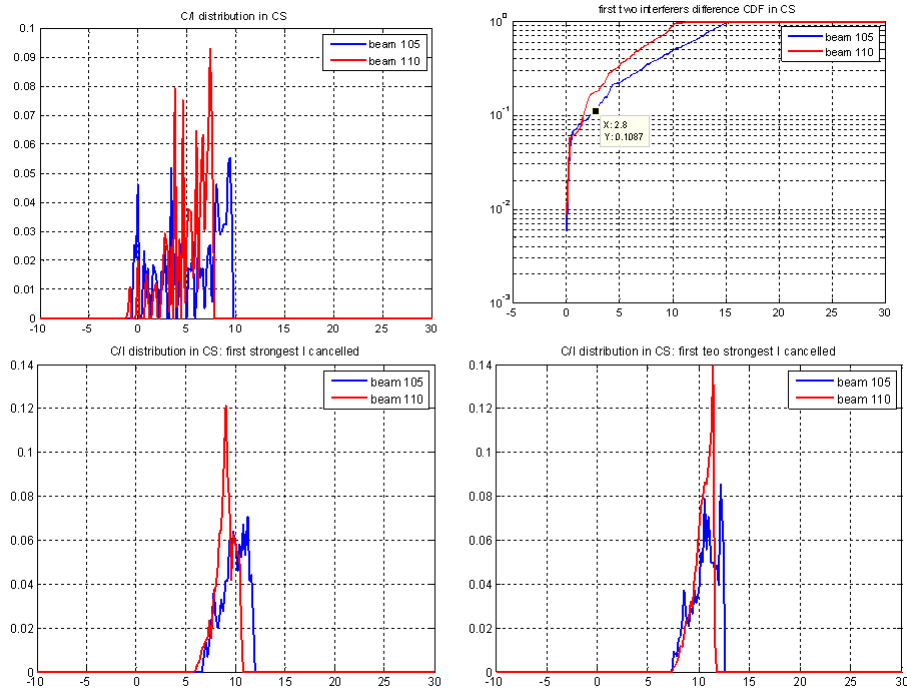
Figure 8. Distribution of interference across the covered area in case: 1) all interferers are present (top-left), 2) the strongest interferer has been removed (bottom-left), 3) the two strongest interferers have been removed (bottom-right). The CDF of the difference between the two strongest interferers across the beam is also shown (top-right).

conclude that the total C/I is mainly limited by the first strongest interferer while the second one has only limited impact on performance. We propose therefore to deal with only one interfering signal while treating the others as noise in order to keep the complexity low. In order to further reduce the complexity we apply just one iteration of the iterative decoding process previously described and shown in Fig. 3 for the case of two interferers. In this way the only modification needed at the decoder side is in the detector, for which the a-priori probability in case of one interferer reduces to:

$$P_{k,s_n} = \sum_{m=0}^{M-1} \exp \left\{ \frac{|y_k - hg^C(t_k)s_n - hg^I(t_k)s_m^I|^2}{2\sigma_{eq}^2} \right\}, \tag{19}$$

M being the cardinality of the interferer's constellation. The correspondent block scheme is shown in Fig. 9.

In order to take into account the influence of the other interferers (which reduces the reliability of the detection) in the received signal's statistics we increase σ_{eq}^2 by several dBs (6 in the following simulations) with respect to the actual variance of the thermal noise σ^2. The optimal choice would be to choose the value of σ_{eq} by estimating the noise-plus-interference power. However in practice keeping a fixed value of the variance can be a good compromise since i) the thermal noise component can be either given by the terminal manufacturer or easily estimated, while the power due to residual interference may not be easy to measure, as the received signal is made up by the sum of the (strong) reference signal, a (possibly strong) dominant interferer and the residual interferer (estimation of the residual interference power in such conditions would increase the complexity of the receiver) and ii) the FER shows little sensibility to the exact value of σ_{eq}. In the simulations presented in the following the signal model described in equations 1-5 has been adopted: all 10 interferers have been simulated including channel code, modulation and channel effect, and scaling the powers according to Table I. We first present the results obtained in AWGN channel and then those for the LMS
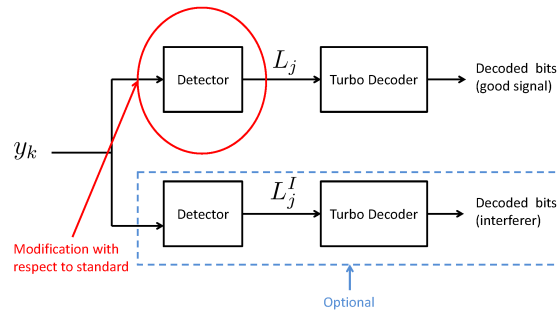
Figure 9. Proposed simplified SIC scheme. Only the strongest interferer is taken into account and no iterative detection/decoding is applied (i.e., reference signal is detected as described in Section 3 and decoded using the turbo decoder specified in [10]). Optionally, also the strongest interfering signal can be decoded.

scenario. The simulation setup for the two cases is depicted in Fig. 10. The simplified scheme shown in Fig. 9 (i.e., the received signal passes through the detector and through the turbo decoder just once) has been used.
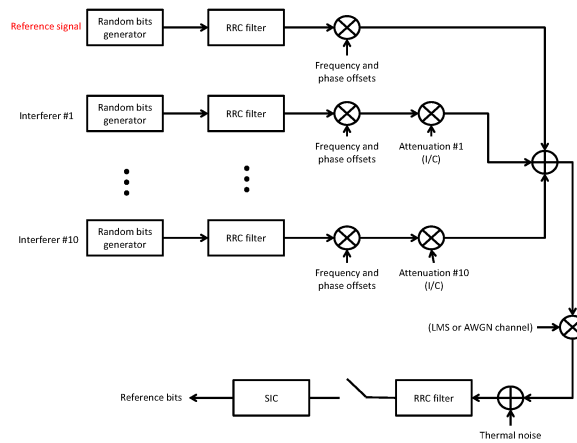
Figure 10. Simulation setup in AWGN and LMS channels.

4.1. AWGN Channel

In figures 11, 12 and 13 we show the FER curves for the simplified SIC in AWGN using the interference pattern detailed in Table I. Different combinations of MODECODs available in the standard [12] have been used, namely QPSK rate 1/3 for all signals in Fig. 11, QPSK with rate 2/5 for all signals in Fig. 12 and QPSK while rate 1/3 for the reference signal and 16 QAM rate 1/3 for interferers are used in Fig. 13.

From the plots it emerges that the target FER of 10^{-3} can be achieved using QPSK modulation in all signals up to rate $2/5$ while if 16 QAM is used in one of (or both) the signals the target FER cannot be achieved for values of C/N of practical interest.

In the following we present the results for an LMS scenario.

4.2. LMS Channel

The channel model used in the simulations presented in the following is a land-mobile satellite (LMS) channel for vehicles moving at a speed of 50 kmph in a suburban environment. A channel realization of 30 minutes (25 km path at 50 kmph) has been used, corresponding to about 2.7×10^4 FEC blocks for bearer F80T025Q1B-L8 (QPSK, rate $1/3$, symbol rate 8400 symbols per second).
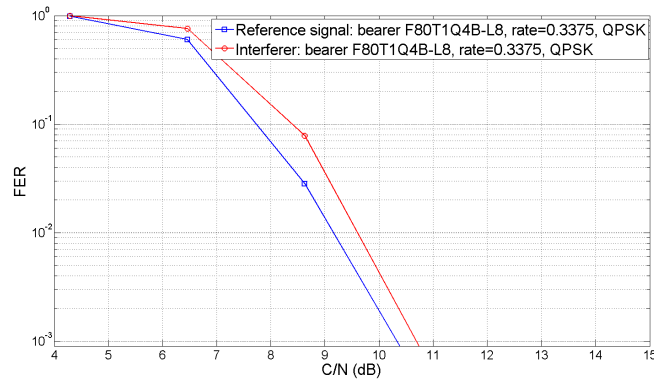
Figure 11. FER in AWGN, simplified MUD. Bearer F80T1Q4B-L8 (QPSK rate $1/3$, symbol rate 33600 sym/sec, roll-off 0.25) is used for all signals. The interference pattern for beam 110 EoB detailed in Table I (worst case scenario) has been used.
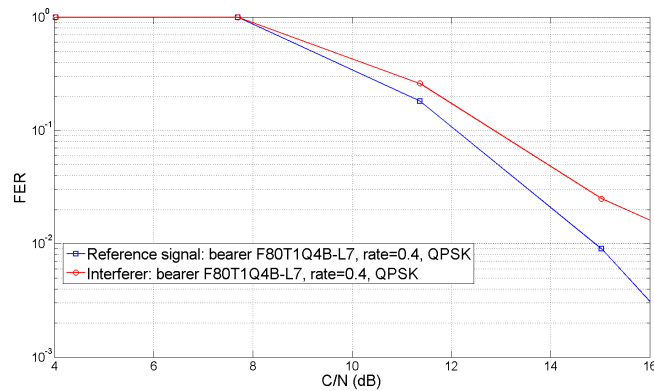

Figure 12. FER in AWGN, simplified MUD. Bearer F80T1Q4B-L7 (QPSK rate $2/5$, symbol rate 33600 sym/sec, roll-off 0.25) is used for all signals. The interference pattern for beam 110 EoB detailed in Table I (worst case scenario) has been used.

A five minutes sample of the channel realization is shown in Fig. 15. The time series has been generated using an LMS channel generator implementing the Perez-Fontan model [22].

In Fig. 15 we show the frame error rate for the reference signal using the proposed simplified SIC scheme. 10 interferers have been considered using the C/I values in Table I. Bearer F80T025Q1B-L8 (QPSK, rate $1/3$) of standard [12] has been adopted for all signals.

Fig. 15 shows that the SIC scheme reaches the target FER of 10^{-3} in all the considered cases, showing a neat enhancement with respect to the case in which no interference cancellation is applied. Thus, it can be seen that decoding is possible in all considered points, while it is not feasible without the MUD algorithm. A relatively high C/N is required in order to fulfill FER requirements in EoB which is due partly to the challenging propagation scenario. As a matter of facts it can be seen in Fig. 15 that, even in case no interference is present in the system, a C/N of about 14 dB is needed to reach a target FER of 10^{-3} We also note that the FER obtained in the LMS channel in case of no interference is almost the same as that in CoB. This is because the total interference level in CoB is low enough to allow for correct decoding even without SIC, which justifies the fact that same performance is achieved by the SIC and the "no IC" (no interference cancellation) schemes.
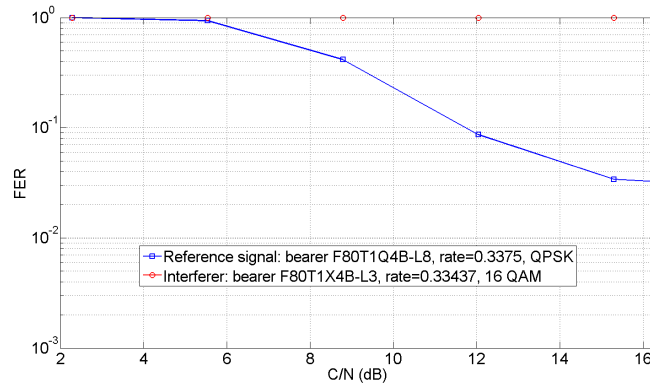
Figure 13. FER in AWGN, simplified MUD. Bearer F80T1Q4B-L8 (QPSK rate $1/3$, symbol rate 33600 sym/sec, roll-off 0.25) is used for the reference signal while bearer F80T1X4B-L3 (16 QAM rate $1/3$, symbol rate 33600 symbols per second , roll-off 0.25) is used for the interferers. Note that rate $1/3$ is the lowest code rate available in [10]). The interference pattern for beam 110 EoB detailed in Table I (worst case scenario) has been used.
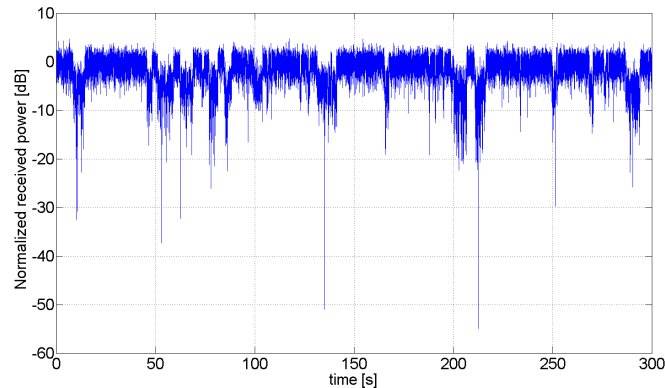

Figure 14. Five minutes sample of the 30 minutes channel series (power in logarithmic scale) used in the simulations. The time series has been generated with a channel simulator implementing the LMS Perez-Fontan model in suburban environment, vehicle speed 50 kmph and satellite elevation 30°.

An interesting outcome of the simulations is that the system results to be interference-limited mainly in the EoB area, while interference has little effect in the CoB area. We also showed that dealing with a single interferer is enough to make decoding possible. We emphasize that these results have been achieved with a limited increase in the receiver complexity, as only the demapper has been modified with respect to the receiver described in [10]. The fact that a C/N larger than 20 dB is needed in EoB could be addressed by using a code with longer codewords (the turbo code of DVB-SH, for instance, has codewords which are an order of magnitude larger than those used in the simulations just presented), an interleaver with an adequate depth or a combination if the two, compatibly with memory and latency constraints in the user terminals.

Finally, we point out that the results in Fig. 5 (more than one detection-decoding iteration) can be easily extended to the case of a single high-power interferer and many low-power interferers, which is the case of the interference scenario described by Table I, as the low-power interferers globally behave similarly to an additional Gaussian noise source. With reference to beam 110 EoB (worst case scenario), for instance, such additional noise source has a power of variance $\sigma_{add}^2 = 0.1763$. Thus, the proposed method with 15 iterations would achieve the target FER at $C/I \simeq 8.1$ dB with a gain of about 2.1 dB with respect to the simplified scheme (simplified SIC) shown in Fig. 9.
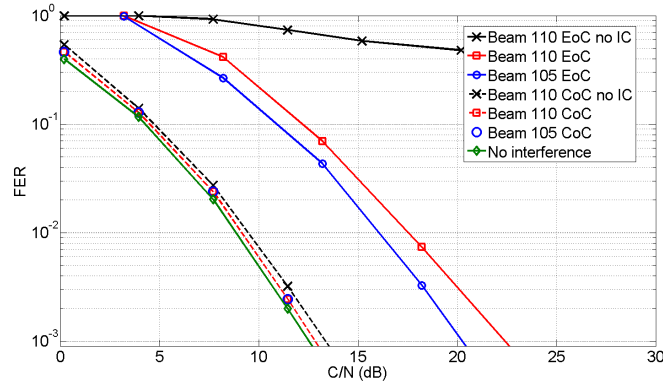
Figure 15. Frame error rate for the reference signal using the simplified SIC scheme with one iteration (one detection and one decoding iteration). A 30 minutes LMS channel series in suburban environment generated according to [23] has been used. 10 interferers have been considered using the C/I values in Table I. Bearer F80T025Q1B-L8 (QPSK, channel code rate $1/3$, symbol rate 8400 symbols per second) of standard [10] has been adopted for all signals.

4.3. Timing Errors

The results presented so far rely on perfect symbol alignment of all signals transmitted by the satellite on the different beams. As in a real system a certain misalignment is likely to be present, we evaluated the impact of alignment (timing) error on the proposed technique. We assume a delay between the ISI-free instants of the reference signal and the ISI-free instants of all the interferers equal to $\tau = X \times T_s$, where T_s is the symbol duration and $X \in (0, 1/2)$ corresponds to the delay normalized to the symbol duration. As in all the other simulations presented so far, SRRC pulse filters with roll off specified in [10] have been used. Frequency and phase offsets have been taken into account and the interference pattern of Fig. 8 has been assumed in AWGN channel. In Fig.
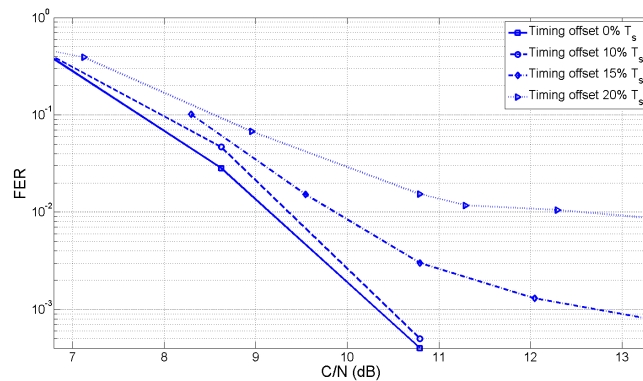

Figure 16. FER in AWGN, simplified MUD, QPSK rate $1/3$ used in all signals. Curves for different relative delays are shown. Delays are expressed in fraction of symbol duration T_s.

16 we show the FER obtained for different relative delays expressed in percentage of the symbol duration. It can be seen how a timing offset of up to 15% allows to achieve the target FER. The loss in SNR for an offset of 15% is slightly larger than 2 dB. If the offset is raised up to 20% the target FER can no longer be achieved within the specified C/N range ($[0 - 20]$ dB).

5. CONCLUSIONS AND DISCUSSION

We studied the application of co-channel soft interference cancellation in multibeam mobile satellite systems with a dense frequency reuse scheme. We took the ETSI standard [12], currently used in commercial satellite systems, as a reference and simulated the beam radiation and the interference patterns using a realistic antenna model, while the calculation of the interference pattern has been carried using a simulator developed by ESA. Due to strong complexity limitations in mobile terminals, we proposed to move part of the complexity to the system level, by aligning signals transmitted over different beams and adding specific signalling information in the global beam. We started from the analysis of the interference levels across the beams selecting two of them as best and worst case scenarios. We applied a serial iterative detection-decoding scheme with optimal symbol detector. We studied the gap between the performance of the proposed iterative scheme and the Shannon bound for successive interference cancellation, showing that most of the loss is due to the non-ideal physical layer considered, while less than an additional dB of loss is introduced by the proposed scheme. In order to keep the complexity at the receiver low we also proposed a simplified scheme in which only the detector is modified with respect to the standard [10]. Our results showed that even under challenging propagation conditions and with strong interference, the simplified scheme leads to interesting results, achieving a target FER of practical interest. We also showed that the proposed scheme can, up to a certain extent, tolerate signals misalignment, achieving the target FER for a timing offset of up to 15%.

The assumption of using the same symbol rate across on all beams may give rise to the objection that different services and different terminal types may require different symbol rates. The assumption of a fixed symbol rate across all beams can be actually relaxed in some cases. Specifically, as it is often the case in real systems, more than one carrier can be assigned to a beam. The solution we propose could be applied also in the case in which, within a beam, different carriers have different symbol rates. For example, given a beam j, let us refer to the number of carriers in the beam as N_c^j. Each of the carriers can have a different symbol rate (and bandwidth). Let us refer to the symbol rate of the i-th carrier on beam j as B_i^j. The low complexity SIC can be applied also in this case provided that the same number of carriers is used in all beams ($N_c^j = N_c^{j'} \ \forall j, j'$) and that carrier i has the same symbol rate ($B_i^j = B_i^{j'} \ \forall j, j'$) and the spectral position in all beams. In this way carriers with different symbol rates could be present in each beam while keeping the complexity at the demodulator low.

Although a single polarization has been considered in the present paper, the same concepts presented here can be extended to a dually polarized system. In this case one possibility is to consider still a two colors scheme in which orthogonality is achieved in the polarization rather than in the frequency domain. Considering dual polarization would double the bandwidth of the system with respect to the single polarization case if the same bandwidth is kept on each of the polarizations. Further studies are needed to assess the impact cross-polar interference would have in such context.

As a final remark, a full-scale study of the impact the proposed method would bring in terms of system throughput and availability, as well as a sensitivity analysis of such impact with respect to the terminal complexity are needed to have a complete picture. Given the vastity of the subject and for a matter of space, we consider such study as an interesting subject for future work.

The view expressed herein can in no way be taken to reflect the official opinion of the European Space Agency.

This is a draft version of the following article: G. Cocco, M. Angelone, A.I. Perez-Neira, Co-Channel Interference Cancellation at the User Terminal in Multibeam Satellite Systems to appear in Wileys International Journal of Satellite Communications and Networking.

REFERENCES

1. J. G. Andrews, "Interference cancellation for cellular systems: a contemporary overview," *IEEE Wireless Comm.*, vol. 12, no. 2, pp. 19–29, 2005.
2. T. M. Cover and J. A. Thomas, *Elements of Information Theory*, second edition ed. John Wiley & Sons, 2006.
3. X. Wang and H. V. Poor, "Iterative (turbo) soft interference cancellation and decoding for coded CDMA," *IEEE Trans. on Commun.*, vol. 47, no. 7, pp. 1046–1061, 1999.
4. M. Kopbayashi, J. Boutros, and G. Caire, "Successive interference cancellation with SISO decoding and EM channel estimation," *IEEE Journal on Selected Areas in Comm.*, vol. 19, no. 8, pp. 1450–1460, 2001.
5. G. Colavolpe, D. Fertonani, and A. Piemontese, "SISO detection over linear channels with linear complexity in the number of interferers," *IEEE Journal of Selected Topics in Signal Processing*, vol. 5, no. 8, pp. 1475–1485, 2011.
6. C. Schlegel, "Achieving the multiple-access capacity of the AWGN channel with iterative processing," in *AESS European Conference on Satellite Telecommunications (ESTEL)*, Rome, Italy, Oct. 2012.
7. B. F. Beidas, H. El-Gamal, and S. Kay, "Iterative interference cancellation for high spectral efficiency satellite communications," *IEEE Trans. on Comm.*, vol. 50, no. 1, pp. 31–36, 2002.
8. M. Moher, W. Zhang, P. Febvre, and J. Rivera-Castro, "Multi-user detection for Inmarsat's BGAN system," in *Advanced Satellite Multimedia Systems conf. (ASMS) and Signal Processing for Space Communications workshop (SPSC)*, Cagliari, Italy, Sep. 2010, pp. 135–140.
9. European Space Agency, "ESA Artes 1 contract 4000106528/12/nl/nr, next generation waveforms for improved spectral efficiency," https://artes.esa.int/projects/next-generation-waveform-improved-spectral-efficiency, 2012-2015.
10. European Telecommunications Standards Institute, "Satellite component of UMTS (S-UMTS) family SL satellite radio interface; part 2: Physical layer specifications; sub-part 1: Physical layer interface," May 2012.
11. A. Barbieri, D. Fertonani, and G. Colavolpe, "Time-frequency packing for linear modulations: spectral efficiency and practical detection schemes," *IEEE Trans. on Commun.*, vol. 57, no. 10, pp. 2951–2959, 2009.
12. European Telecommunications Standards Institute, "Satellite component of UMTS (S-UMTS) family SL satellite radio interface; part 1: General specifications; sub-part 3: Satellite radio interface overview," May 2011.
13. International Telecommunications Union - Radiocommunications Sector, "Propagation data and prediction methods requred for the design of Earth-space telecommunication systems: methods requred for the design of Earth-space telecommunication systems," Reccomendation ITU-R P.618-10 (10/2009), Oct. 2009.
14. Inmarsat, "Broadband Global Area Network (BGAN)," http://www.inmarsat.com/services/bgan.
15. Satsoft, http://www.satsoft.com/.
16. M. Feder and E. Weinstein, "Parameter estimation of superimposed signals using the EM algorithm," *IEEE Trans. on Acoustics, Speech and Signal Processing*, vol. 36, no. 4, pp. 477–489, Apr. 1988.
17. G. Cocco, N. Alagha, C. Ibars, and S. Cioni, "Practical issues in multi-user physical layer network coding," in *IEEE Advanced Satellite Mobile Systems conf. (ASMS)*, Baiona, Spain, Sep. 2012.
18. K. Zidane, J. Lacan, M.-L. Boucheret, and C. Poulliat, "Improved channel estimation for interference cancellation in random access methods for satellite communications," in *Advanced Satellite Multimedia Systems Conference (ASMS), to appear*, Livorno, Italy, Sep. 2014.
19. European Space Agency, "NGWISE project technical Annex B: Technologies, models and requirements for the work of RG2 on MSS," 2013.
20. G. Ungerboeck, "Channel coding with multilevel/phase signals," *IEEE Trans. on Info. Theo.*, vol. 28, no. 1, pp. 55–67, Jan. 1982.
21. C. E. Shannon, "A mathematical theory of communication," *The Bell System Technical Journal*, vol. 27, pp. 379–423 and 623–656, July and Oct. 1948.
22. F. Perez-Fontan, M. A. Vazquez-Castro, S. Buonomo, J. P. Poiares-Baptista, and B. Arbesser-Rastburg, "S-band LMS propagation channel behaviour for different environments, degrees of shadowing and elevation angles," *IEEE Trans. on Broadcasting*, vol. 44, no. 1, pp. 40–76, Mar. 1998.
23. F. Perez-Fontan, A. Mayo, D. Marote, R. Prieto-Cerdeira, P. Marino, F. Machado, and N. Riera, "Review of generative models for the narrowband land mobile satellite propagation channel," *Int'l Journal of Satellite Comm. and Networking*, vol. 26, pp. 291–316, 2008.